iPEP: peptides designed and selected for interfering with protein interaction and function

Jody M. Mason*[1], Kristian M. Müller* and Katja M. Arndt*†‡[2]

*Department of Biology, Albert-Ludwigs University of Freiburg, D79104 Freiburg, Germany, †Center for Biological Signaling Studies (bioss), Albert-Ludwigs University of Freiburg, D79104 Freiburg, Germany, and ‡FRIAS, School of Life Sciences – LIFENET, Albert-Ludwigs University of Freiburg, Albertstrasse 19, 79104 Freiburg, Germany

Abstract

Semi-rational design is combined with PCAs (protein-fragment complementation assays) and phage-display screening techniques to generate a range of iPEPs (interfering peptides) that target therapeutically relevant proteins with much higher interaction stability than their native complexes. PCA selection has been improved to impose a competitive and negative design initiative on the library screen, thus simultaneously improving the specificity of assay 'winners'. The folding pathways of designed pairs imply that early events are dominated by hydrophobic collapse and helix formation, whereas later events account for the consolidation of more intricate intermolecular electrostatic interactions.

Introduction

Is it possible to design proteins that can recognize and bind to each other in both a stable and specific manner? Answering this question is of importance not only in mapping of protein networks, but also in devising iPEPs (interfering peptides) and later peptidomimetic antagonists able to mimic natural proteins by binding and sequestering interaction partners. The ability to do this at will should further our goal in understanding how protein networks function, and will generate sequences capable of sequestering proteins that behave abnormally and give rise to a pathogenic phenotype.

Coiled coils

We seek to answer this question by focusing our research efforts on parallel dimeric coiled-coil motifs. The coiled coil is a particularly attractive motif to study since it is one of the most simplistic examples of quaternary structure, but is highly specific, and is found in a diverse range of proteins [1–4]. Indeed, it is found in 3–5% of the entire coding sequence [5] where it serves in transcriptional control [6], muscle contraction [7], viral infection [8,9], cell signalling [10], molecular chaperones [11] and fertilization [12], and is therefore the ideal test bed for specificity. It contains a regular repeating unit of seven amino acids (the heptad repeat; Figures 1A and 1B) characterized by distinctive hydrophobic/hydrophilic residues. The patterning of these charged and hydrophobic residues can have profound effects on the stability and specificity, as well as orientation and oligomeric state, of the resultant interactions [13–15].

AP-1 (activator protein-1)

Our focus has resided on the transcription factor AP-1 (Figure 1C). AP-1 dimer formation is mediated by members of Jun (c-Jun, JunB and JunD) and Fos (c-Fos, FosB, Fra1 and Fra2), with DNA binding occurring at a specific consensus sequence (TGAGTCA), known as the TRE [PMA ('TPA')-responsive element]. Jun and Fos members contain an N-terminal transactivation domain, a basic region for recognizing the consensus sequence and a leucine zipper or coiled-coil region responsible for mediating homo- (for Jun members) or hetero-dimerization. Such transcription factors, known as bZIP (basic leucine zipper) proteins, are found at the end of several cell signalling cascades. AP-1 has been implicated in numerous cancers and is therefore thought to represent a legitimate therapeutic target. However, AP-1 can also have antiproliferative properties, depending on subunit composition, transcription level, post-translational modification (e.g. phosphorylation) and interaction with other proteins [e.g. JNK (c-Jun N-terminal kinase)]; this is clear from the abundance of different AP-1 family members in different types of cancer. For example, c-Jun is central in skin and liver tumours, whereas JunB and JunD have very poor transactivation domains, weak transforming activities, and may have an alternative role to play. Fra1 and Fra2 have weak transactivation domains, but are found in lung and epithelial tumours, possibly by dimerizing with other family members possessing intact transactivation domains [16]. In inhibiting inappropriate AP-1 formation, or permitting correct AP-1 pairings by sequestering potential partners, specific AP-1 dimers can be targeted, generating sequences that are of both analytical and therapeutic use. In our opinion, the

Key words: activator protein-1 (AP-1), basic leucine zipper (bZIP), interfering peptide, protein-fragment complementation assay (PCA), protein–protein interaction, semi-rational design.

Abbreviations used: AP-1, activator protein-1; bCIPA, basic coiled-coil interaction prediction algorithm; bHLHZip, basic helix–loop–helix leucine zipper; bZIP, basic leucine zipper; CANDI, competitive and negative design initiative; EMSA, electrophoretic mobility-shift assay; iPEP, interfering peptide; mDHFR, murine dihydrofolate reductase; Mip, Myc-interfering peptide; PCA, protein-fragment complementation assay; TRE, PMA ('TPA')-responsive element.

[1]**Present address:** Department of Biological Sciences, University of Essex, Wivenhoe Park, Colchester, Essex CO4 3SQ, U.K.

[2]**To whom correspondence should be addressed (email katja@biologie.unifreiburg.de).**

Figure 1 | **Schematic representation and structure of the paralled dimeric coiled-coil motif**

(**A**) Helical wheel diagram looking down the helix axis from the N- to the C-terminus. Heptad positions are labelled **a**–**g** and **a′**–**g′** respectively. Positions **a**, **d**, **e** and **g** are colour-coded. Modified from [18] with permission. © 1999 Nature. (**B**) In the side view, the helical backbones are represented by cylinders, the side chains by knobs, and the path of the polypeptide chain is indicated by a line wrapped around the cylinders. For simplicity, the supercoiling of the helices is not shown. While residues at positions **a** (purple) and **d** (blue) make up the hydrophobic interface, residues at positions **e** (orange) and **g** (red) pack against the hydrophobic core. They can participate in interhelical electrostatic interactions between residue *i* (**g** position) of one helix and residue *i′* + 5 of the other helix (**e′** position, belonging to the next heptad), as indicated by the hatched bars. Also indicated is the core **a** position (green), which is often occupied by polar residues mediating strand-paining specificity. Modified from [14] with permission. © 2000 Elsevier. (**C**) The structure of the DNA-bound c-Jun–c-Fos AP-1 bZIP domain (PDB co-ordinates 1FOS [6]). The Figure was created using PyMOL (DeLano Scientific; http://pymol.sourceforge.net/).

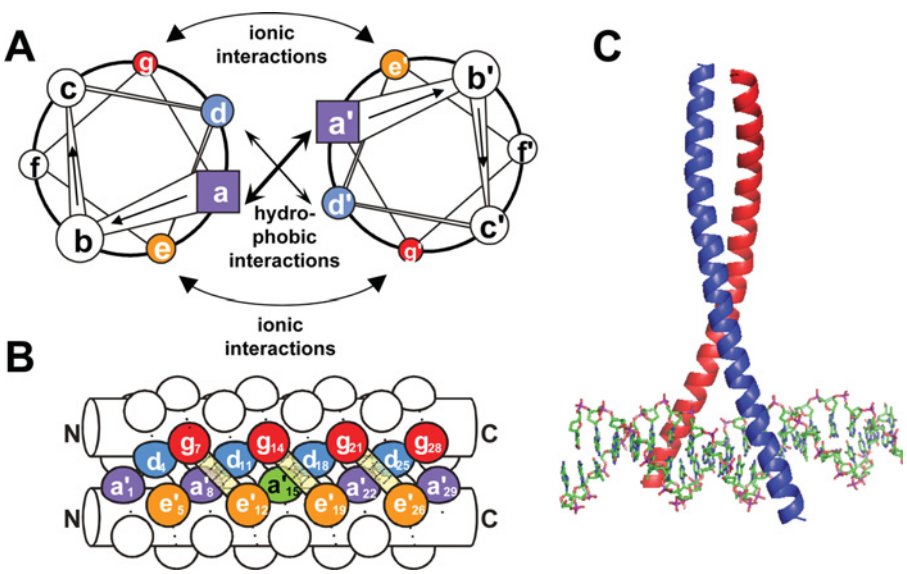

most efficient, as yet untested, way to do this is via the dimerization-driving coiled-coil domain.

Selection of JunW and FosW using a PCA (protein-fragment complementation assay) system

We first sought to characterize all possible Jun–Fos coiled-coil interactions by synthesizing the nine homologues of the AP-1 leucine zipper region, and consequently found electrostatic **e**–**g** pairings, core residue pairings and helical propensity to be dominating factors in determining coiled-coil stability [17]. In addition, two libraries designed to target c-Jun and c-Fos were synthesized and screened, using Fos and Jun families respectively as starting points in the design. These libraries were constructed at the genetic level with oligonucleotides containing semi-randomized codons corresponding to residue options within the heptad repeats. These semi-randomized positions coded for mostly interfacial residues crucial for dimerization and stability and used numerous potential residue options (including most wild-type residues). Importantly, unintuitive residue selections, arising from retained wild-type amino acids and those appearing to contribute poorly to overall stability (from homologues), were included as well. Often away from the interface, these can fulfil poorly understood roles in intramolecular interactions, helical propensity and solubility, generating improved overall stability. The libraries were screened *in vivo* for an interaction with a partner helix by using a PCA system based on mDHFR (murine dihydrofolate reductase) [14,18]. In this system, one half of mDHFR is genetically fused to the target, and the second half of mDHFR is fused to the protein library. Only library members binding to the target will bring the two halves of DHFR together, render the enzyme active and result in a bacterial colony under selective conditions [14,18]. Subsequent growth competitions under selective conditions enriched two 'winning' peptides (iPEPs), termed FosW and JunW, targeting c-Jun and c-Fos respectively [17]. These 37-mer peptides were analysed regarding both their stabilities and specificities. The new dimeric coiled coils, c-Jun–FosW and c-Fos–JunW, displayed remarkable T_m values of 63 and 44°C, compared with only 16°C for the wild-type coiled-coil c-Jun–c-Fos, thus fulfilling the criteria of higher stability. The impressive 70000-fold K_d improvement for c-Jun–FosW is largely due to optimized core packing, α-helical propensity and electrostatics. In contrast, owing to a poor c-Fos core, c-Fos–JunW dimerizes with lower affinity. However, the T_m far exceeded wild-type c-Jun–c-Fos and

averaged JunW and c-Fos, indicating a preference over either homodimer. In addition, as PCA is carried out entirely *in vivo*, only soluble, non-aggregating, protease-resistant, stable inhibitors that bind their targets with high efficacy are selected. Sequestering one half of AP-1 with such potency should strongly and indefinitely inhibit transcription of the target gene.

bCIPA (basic coiled-coil interaction prediction algorithm)

One surprising outcome of the above study was the selection of sequences with much improved α-helical propensity over homologues, despite not being a factor in the initial library design criteria. With this in mind, we generated thermal melting data for all 45 possible homo- and hetero-dimeric interactions between homologues and 'winners' to permit broader inferences regarding FosW and JunW specificity, as well as attempting to relate sequence to stability based on thermal melting data alone. Achieving this permitted a quantitative ranking of bZIP stability based only on sequence data. To this end, we compiled a method for predicting interaction of parallel, dimeric coiled coils, using our T_m data as a training set, and applying it to 59 bZIP proteins previously reported [19]. Our algorithm, unlike others to date, considers helix propensity, which is found to be integral in coiled-coil stability, in addition to electrostatic ***e–g*** and core **a–a′** and **d–d′** residue interactions [20,21]. Indeed, in applying the algorithm to all 59^2 bZIP interactions, we were able to correctly identify 97% of all strong interactions and 95% of all non-interacting pairs [17,22] (http://www.molbiotech.uni-freiburg.de/bCIPA/).

Selection of $JunW_{CANDI}$ using a CANDI (competitive and negative design initiative)

An outcome of the previous study was that, although increased stability is relatively straightforward to design and select for, it is much harder to confer a specific interaction while maintaining this high interaction stability. Designing peptide-based inhibitors to bind with both high affinity and specificity to pathogenic proteins implicated in disease is of utmost importance, and promises to yield important rules. Designed inhibitors arising from 'single-state' approaches may meet their objective in binding to their target with desired affinity. The advantage, however, of *in vivo*-derived inhibitors is increased target specificity. This so-called negative or 'multistate' design is imperative in deriving high-affinity, yet specific, peptide-based drugs. We therefore devised an *in vivo* selection of specific and stable interactions by expressing homologous peptides (that lack DHFR-fragment fusion), which then compete with protein libraries for an interaction with a target molecule during PCA selection [23]. Library members binding to their target, and promoting cell growth, must outcompete competitor interactions with the target (i.e. competition) and evade binding to the competitors (i.e. negative design). We term this a 'competitive and negative design initiative', or CANDI (Figure 2A). By combining CANDI with PCA selection, we observed major specificity improvements, by driving selection of winning library members that bind their target with maximum efficacy, ensuring that otherwise energetically accessible alternatives are inaccessible [23]. CANDI–PCA has been used with libraries targeted at coiled-coil regions of oncogenic AP-1 components c-Jun and c-Fos. We demonstrated that comparable hydrophobic and electrostatic contributions in desired species are compromised in non-desired species when CANDI is executed, demonstrating that both core and electrostatic residues are required to direct specific interactions. Major energetic differences (5.6 kcal/mol; 1 kcal $\approx$ 4.184 kJ) are observed between desired and non-desired interaction stabilities for a CANDI–PCA-derived peptide relative to a conventional PCA-derived helix, with significantly higher stability (3.2 kcal/mol) than the wild-type c-Jun–c-Fos complex (Figure 2B). As a negative control, a library lacking a residue repertoire able to generate a specific and stable helix was also tested.

Comparison of PCA with phage display

Peptides were selected from the same parent library as the PCA-selected JunW peptide using the phage-display technique to permit a direct comparison of selected sequences and the ability of these sequences to disrupt the c-Fos–c-Jun interaction [22]. Explicitly, a c-Jun-based library was screened to enrich for peptides that disrupt the AP-1 complex by binding to the c-Fos coiled-coil domain. Interestingly, phage display identified one helix, $JunW_{Ph1}$ (phage-display-selected winning peptide targeting c-Fos), which differed in only two of ten randomized positions relative to JunW (PCA-selected winning peptide targeting c-Fos). Phage-selected peptides revealed higher affinity for c-Fos than wild-type c-Jun, harbouring a T_m of 53°C, compared with 16°C for c-Jun–c-Fos or 44°C for c-Fos–JunW. Using PCA growth assays in the presence of c-Jun as a competitor, phage-selected $JunW_{Ph1}$ conferred a shorter generation time than JunW. Bacterial growth was barely detectable using $JunW_{Ph1}$ as a competitor for the wild-type c-Jun–c-Fos interaction, indicating efficient c-Fos removal from the dimeric wild-type complex. Importantly, all inhibitory peptides were able to interfere successfully with DNA binding as demonstrated in gel-shift assays (Figure 3). These selected sequences were used to further refine '*bCIPA*' in distinguishing interacting from non-interacting coiled-coil sequences [22].

Folding of Jun–Fos AP-1 coiled-coil motifs

A further insight into the structural determinants of stability arose by dissecting the folding pathway of four c-Jun leucine zipper variants that bind with high affinity to c-Fos [24]. These encompassed a PCA-selected winner (JunW) [17], a phage-display-selected winner ($JunW_{Ph1}$) [22] and two intermediate mutants. The enriched winners differ from each

Figure 2 | **Simultaneous selection for complex stability and specificity**

(**A**) Conceptual diagram highlighting CANDI, which has been applied using the PCA system. Only favourable and specific interactions between a library member (gold) and target (blue) will reconstitute the mDHFR enzyme and thus will give rise to a bacterial colony under selective conditions (outcome 1). Conventional PCA already disfavours homodimers (outcomes 2 and 3), whereas CANDI–PCA enhances this effect by including additional constraints. Library members that have a lower binding constant for the target than the target–competitor interaction (outcome 4) or that bind preferentially to the competitor (red; outcome 5) are detrimental inhibitors and will result in no or retarded cell growth. In the case of low-affinity binding (a combination of outcome 1 with undesired outcomes 2 and/or 4) or non-specific binding (a combination of 1 with 3 and/or 5), the colony will be outgrown in subsequent growth competitions by library members of comparable or better affinity, but higher specificity. (**B**) PCA selection without (left) and with (right) CANDI. Thermal stability of peptide pairs was measured by using temperature dependence of the CD signal at 222 nm. Colours correspond to PCA outcomes described in (**A**). In PCA without CANDI, the desired c-Fos–JunW (green), although clearly preferential over wild-type c-Jun–c-Fos (cyan) or c-Fos alone (blue), displays a lower T_m than competing complexes JunW–JunW (orange) and c-Jun–JunW (red). The stability of these complexes, however, is relieved in PCA–CANDI, where c-Jun is present as a competitor, resulting in both stability and specificity for the desired c-Fos–JunW_{CANDI} complex (green). Adapted with permission from [23]. © 2007 American Chemical Society.

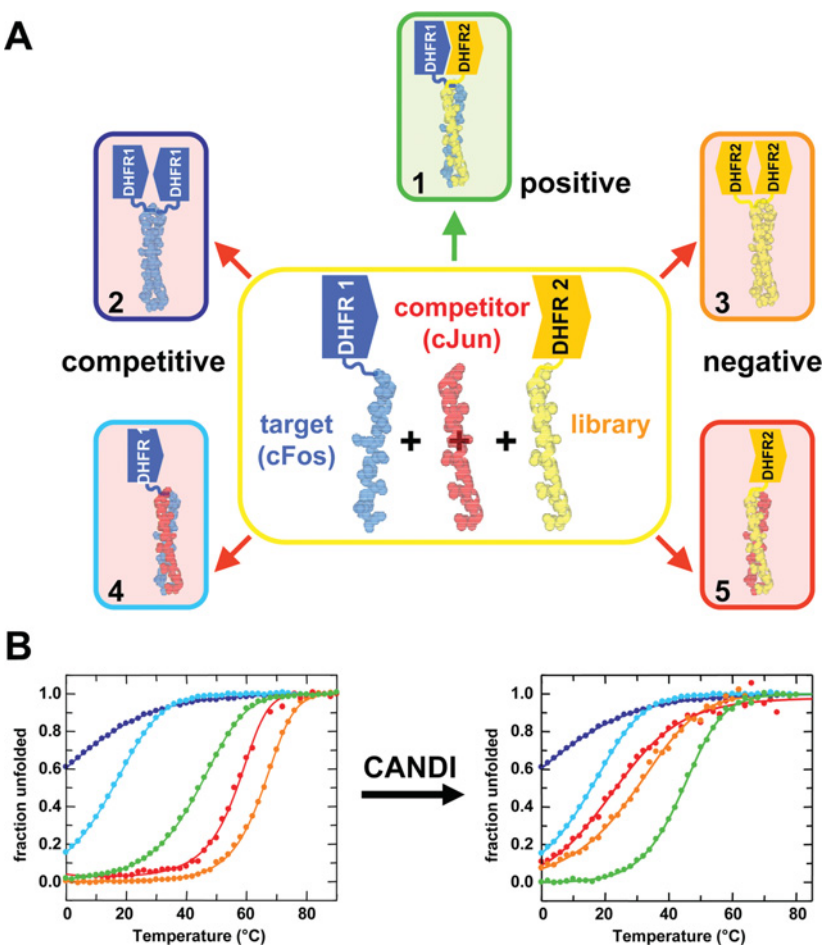

other in only two of ten semi-randomized positions (Q21R and E23K) with ΔT_m values of 28 and 37°C over wild-type. c-Fos–JunW, c-Fos–JunW_{Ph1} and the two intermediate mutants (c-Fos–JunW_{Q21R} and c-Fos–JunW_{E23K}) display biphasic kinetics in the folding direction, indicating the existence of a folding intermediate. The first reaction phase is fast and concentration-dependent, showing that the intermediate is readily populated and dimeric. The second phase is independent of concentration and is exponential. In contrast, in the unfolding direction, all molecules display two-state kinetics [24]. Collectively, this implies a transition state between unfolded helices and a dimeric intermediate that is readily traversed in both directions. We have demonstrated that the added stability of c-Fos–JunW_{Ph1} relative to c-Fos–JunW is achieved via a combination of kinetic rate changes; c-Fos–JunW_{E23K} has an increased initial dimerization rate, prior to the major transition state barrier, whereas c-Fos–Jun-W_{Q21R} displays a decreased unfolding rate. The former

Figure 3 | EMSA analysis of DNA-bound c-Jun–c-Fos or Myc–Max in the absence or presence of iPEPs

GFP (green fluorescent protein)–His-tagged bZIP domains of Jun and Fos (100 ng each per lane) bound TRE DNA (TGACTCA, lane 2) and were efficiently inhibited by phage-selected $JunW_{Ph1}$ (2- and 20-fold excess, lanes 3 and 4) but only marginally by the coiled-coil domain of c-Jun (lanes 5 and 6). $JunW_{Ph1}$ had no effect on Myc–Max DNA binding (lanes 7 and 8). His-tagged bHLHZip domains of Myc and Max (50 ng each) bound E-box DNA (CACGTG, lane 9), but not TRE DNA (lane 15), and were replaced by inhibitory aMip (lanes 10–13) and aMax (lane 14) (molar ratio of inhibitor to Myc–Max of 0.25:1–2:1). Reproduced from [22] (© 2008 Elsevier) and [26] (© 2008 John Wiley and Sons) with permission.

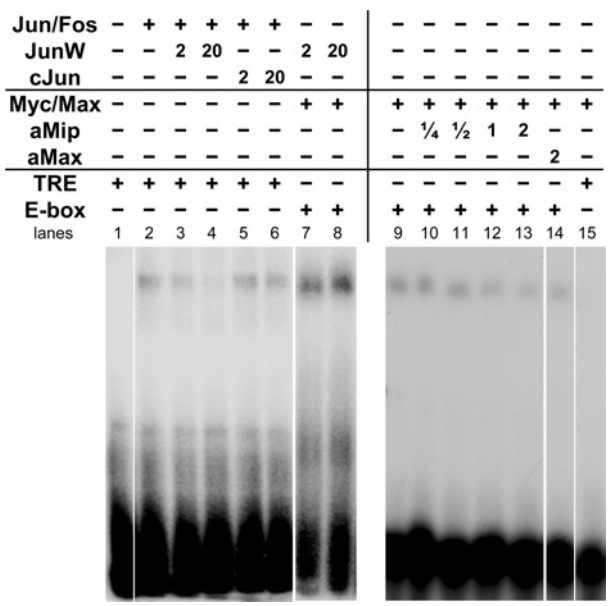

implies that improved hydrophobic burial and helix-stabilizing mutations exert their effect on the initial, rapid, monomer collision event. In contrast, electrostatic interactions exert their effect late in the folding pathway. Although our focus was on the leucine zipper region of the oncogenic transcription factor AP-1, coiled coils are ubiquitous and highly specific in their recognition of partners. Consequently, generating kinetics-based rules to predict and engineer their stability is of major significance in peptide-based drug design and nanobiotechnology.

Extending PCA to other therapeutically relevant targets: the Myc–Max system

c-Myc is one of the most frequently deregulated oncogenes in human cancers, and recent studies showed that even brief inactivation of Myc can be sufficient to induce tumour regression or loss [25]. Consequent inactivation of Myc provides a novel therapeutic opportunity, since dimerization of Myc with Max is crucial for its carcinogenic function. Two strategies were applied in which the coiled-coil motif responsible for mediating dimer formation was targeted with iPEPs: a dominant-negative human Max sequence (Max) and a peptide selected from a genetic library [Mip (Myc-interfering peptide)] [26,27]. Both iPEPs form coiled coils and were fused to an acidic extension [28] interacting with the basic DNA-binding region of human Myc (aMax, aMip). The genetic library was obtained by semi-rational design randomizing residues important for interaction, and selection was carried out using PCA. The peptides aMip and aMax easily outcompeted the human bHLHZip (basic helix–loop–helix leucine zipper) Myc–Max interaction and successfully interfered with the DNA binding of the complex, as verified by EMSA (electrophoretic mobility-shift assay; Figure 3). Both iPEPs exhibited higher T_m values ($\Delta T_m = 13$ and 15°C) upon interaction with Myc compared with wild-type Max. The inhibitory effect of the two iPEPs on human Myc–Max activity makes them promising molecules for analytical and therapeutic Myc-directed research.

Conclusions

PCA and phage display combined with semi-rational design has been used to demonstrate that generating peptides capable of binding and sequestering a range of coiled-coil interactions is an entirely achievable goal. We have increased the stringency of PCA selection by using CANDI to confer specificity as well as stability on the resulting protein–protein interaction, such that the energy barrier between desired and non-desired species is maximized. We have additionally dissected the free energy of the folding pathway of Jun–Fos variants to glean new rules that will aid in the design of stable and specific future antagonists. These rules include introduction of hydrophobic and/or high helical propensity residues to increase the folding rate of coiled-coil formation, as well as engineering intermolecular electrostatic interactions to decelerate the unfolding rate of preformed interactions. Lastly, PCA has been applied to therapeutically relevant systems to generate iPEPs capable of releasing bound DNA from the Jun–Fos bZIP protein and the Myc–Max bHLHZip protein. We aim to collate techniques and rules generated from existing peptides to design future variants, and to demonstrate *in vivo* efficacy. The overall goal is to harness negative protein design to generate specific and therapeutically relevant peptides, peptides in nanobiotechnological design, peptide-based drugs capable of functioning *in vitro* and *in vivo*, and proteins able to act with minimal cross-talk to homologues or analogues.

This work was supported by the Emmy-Noether programme of the DFG (Deutsche Forschungsgemeinschaft; Ar 373/1-1 and 1-2), by the José Carreras Leukemia Foundation (DJCLS R 06/12) and by the Excellence Institute of the German Federal and State Governments, (EXC 24).

References

1 Yu, Y.B. (2002) Coiled-coils: stability, specificity and drug delivery potential. Adv. Drug Deliv. Rev. **54**, 1113–1129
2 Mason, J.M. and Arndt, K.M. (2004) Coiled coil domains: stability, specificity and biological implications. ChemBioChem **5**, 170–176

3 Woolfson, D.N. (2005) The design of coiled-coil structures and assemblies. Adv. Protein Chem. **70**, 79–112
4 Mason, J.M., Müller, K.M. and Arndt, K.M. (2007) Considerations in the design and optimization of coiled coil structures. Methods Mol. Biol. **352**, 35–70
5 Wolf, E., Kim, P.S. and Berger, B. (1997) MultiCoil: a program for predicting two- and three-stranded coiled coils. Protein Sci. **6**, 1179–1189
6 Glover, J.N. and Harrison, S.C. (1995) Crystal structure of the heterodimeric bZIP transcription factor c-Fos–c-Jun bound to DNA. Nature **373**, 257–261
7 Brown, J.H., Cohen, C. and Parry, D.A. (1996) Heptad breaks in α-helical coiled coils: stutters and stammers. Proteins **26**, 134–145
8 Xu, Y., Zhu, J., Liu, Y., Lou, Z., Yuan, F., Cole, D.K., Ni, L., Su, N., Qin, L., Li, X. et al. (2004) Characterization of the heptad repeat regions, HR1 and HR2, and design of a fusion core structure model of the spike protein from severe acute respiratory syndrome (SARS) coronavirus. Biochemistry **43**, 14064–14071
9 Bianchi, E., Finotto, M., Ingallinella, P., Hrin, R., Carella, A.V., Hou, X.S., Schleif, W.A., Miller, M.D., Geleziunas, R. and Pessi, A. (2005) Covalent stabilization of coiled coils of the HIV gp41 N region yields extremely potent and broad inhibitors of viral infection. Proc. Natl. Acad. Sci. U.S.A. **102**, 12903–12908
10 Sharma, V.A., Logan, J., King, D.S., White, R. and Alber, T. (1998) Sequence-based design of a peptide probe for the APC tumor suppressor protein. Curr. Biol. **8**, 823–830
11 Siegert, R., Leroux, M.R., Scheufler, C., Hartl, F.U. and Moarefi, I. (2000) Structure of the molecular chaperone prefoldin: unique interaction of multiple coiled coil tentacles with unfolded proteins. Cell **103**, 621–632
12 Kitamura, K., Tanaka, H. and Nishimune, Y. (2005) The RING-finger protein haprin: domains and function in the acrosome reaction. Curr. Protein Pept. Sci. **6**, 567–574
13 Harbury, P.B., Zhang, T., Kim, P.S. and Alber, T. (1993) A switch between two-, three-, and four-stranded coiled coils in GCN4 leucine zipper mutants. Science **262**, 1401–1407
14 Arndt, K.M., Pelletier, J.N., Müller, K.M., Alber, T., Michnick, S.W. and Plückthun, A. (2000) A heterodimeric coiled-coil peptide pair selected *in vivo* from a designed library-versus-library ensemble. J. Mol. Biol. **295**, 627–639
15 Arndt, K.M., Pelletier, J.N., Müller, K.M., Plückthun, A. and Alber, T. (2002) Comparison of *in vivo* selection and rational design of heterodimeric coiled coils. Structure **10**, 1235–1248
16 Eferl, R. and Wagner, E.F. (2003) AP-1: a double-edged sword in tumorigenesis. Nat. Rev. Cancer **3**, 859–868
17 Mason, J.M., Schmitz, M.A., Müller, K.M. and Arndt, K.M. (2006) Semi-rational design of Jun–Fos coiled coils with increased affinity: universal implications for leucine zipper prediction and design. Proc. Natl. Acad. Sci. U.S.A. **103**, 8989–8994
18 Pelletier, J.N., Arndt, K.M., Plückthun, A. and Michnick, S.W. (1999) An *in vivo* library-versus-library selection of optimized protein–protein interactions. Nat. Biotechnol. **17**, 683–690
19 Newman, J.R. and Keating, A.E. (2003) Comprehensive identification of human bZIP interactions with coiled coil arrays. Science **300**, 2097–2101
20 Krylov, D., Barchi, J. and Vinson, C. (1998) Inter-helical interactions in the leucine zipper coiled coil dimer: pH and salt dependence of coupling energy between charged amino acids. J. Mol. Biol. **279**, 959–972
21 Acharya, A., Rishi, V. and Vinson, C. (2006) Stability of 100 homo and heterotypic coiled coil a–a′ pairs for ten amino acids (A, L, I, V, N, K, S, T, E and R). Biochemistry **45**, 11324–11332
22 Hagemann, U.B., Mason, J.M., Müller, K.M. and Arndt, K.M. (2008) Selectional and mutational scope of peptides sequestering the Jun–Fos coiled-coil domain. J. Mol. Biol. **381**, 73–88
23 Mason, J.M., Müller, K.M. and Arndt, K.M. (2007) Positive aspects of negative design: simultaneous selection of specificity and interaction stability. Biochemistry **46**, 4804–4814
24 Mason, J.M., Hagemann, U.B. and Arndt, K.M. (2007) Improved stability of the Jun–Fos activator protein-1 coiled coil motif: a stopped-flow circular dichroism kinetic analysis. J. Biol. Chem. **282**, 23015–23024
25 Felsher, D.W. (2004) Reversibility of oncogene-induced cancer. Curr. Opin. Genet. Dev. **14**, 37–42
26 Jouaux, E.M., Schmidtkunz, K., Müller, K.M. and Arndt, K.M. (2008) Targeting the c-Myc coiled coil with interfering peptides. J. Pept. Sci. **14**, 1022–1031
27 Krylov, D., Kasai, K., Echlin, D.R., Taparowsky, E.J., Arnheiter, H. and Vinson, C. (1997) A general method to design dominant negatives to bHLHZip proteins that abolish DNA binding. Proc. Natl. Acad. Sci. U.S.A. **94**, 12274–12279

Received 11 August 2008
doi:10.1042/BST0361442